

Expansion and Characterization of Neonatal Cardiac Pericytes Provides a Novel Cellular Option for Tissue Engineering in Congenital Heart Disease

Elisa Avolio, PhD;* Iker Rodriguez-Arabaolaza, BSc;* Helen L. Spencer, PhD;* Federica Riu, PhD; Giuseppe Mangialardi, MD, PhD; Sadie C. Slater, PhD; Jonathan Rowlinson, MSc; Valeria V. Alvino, MSc; Oluwasomdotun O. Idowu, BSc; Stephanie Soyombo, BSc; Atsuhiko Oikawa, PhD; Megan M. Swim, MSc; Cherrie H. T. Kong, PhD; Hongwei Cheng, PhD; Huidong Jia, MD, PhD; Mohamed T. Ghorbel, PhD; Jules C. Hancox, BSc, PhD, FSB; Clive H. Orchard, DSc, PhD, FSB; Gianni Angelini, MD; Costanza Emanuelli, PhD; Massimo Caputo, MD, FRCS; Paolo Madeddu, MD, FAHA

Background—Living grafts produced by combining autologous heart-resident stem/progenitor cells and tissue engineering could provide a new therapeutic option for definitive correction of congenital heart disease. The aim of the study was to investigate the antigenic profile, expansion/differentiation capacity, paracrine activity, and pro-angiogenic potential of cardiac pericytes and to assess their engrafting capacity in clinically certified prosthetic grafts.

Methods and Results—CD34^{pos} cells, negative for the endothelial markers CD31 and CD146, were identified by immunohistochemistry in cardiac leftovers from infants and children undergoing palliative repair of congenital cardiac defects. Following isolation by immunomagnetic bead-sorting and culture on plastic in EGM-2 medium supplemented with growth factors and serum, CD34^{pos}/CD31^{neg} cells gave rise to a clonogenic, highly proliferative (>20 million at P5), spindle-shape cell population. The following populations were shown to express pericyte/mesenchymal and stemness markers. After exposure to differentiation media, the expanded cardiac pericytes acquired markers of vascular smooth muscle cells, but failed to differentiate into endothelial cells or cardiomyocytes. However, in Matrigel, cardiac pericytes form networks and enhance the network capacity of endothelial cells. Moreover, they produce collagen-1 and release chemo-attractants that stimulate the migration of c-Kit^{pos} cardiac stem cells. Cardiac pericytes were then seeded onto clinically approved xenograft scaffolds and cultured in a bioreactor. After 3 weeks, fluorescent microscopy showed that cardiac pericytes had penetrated into and colonized the graft.

Conclusions—These findings open new avenues for cellular functionalization of prosthetic grafts to be applied in reconstructive surgery of congenital heart disease. (*J Am Heart Assoc.* 2015;4:e002043 doi: 10.1161/JAHA.115.002043)

Key Words: cells • congenital heart defects • grafting • myocardium • pediatrics

Congenital heart disease (CHD) is the most common type of birth defect, with a reported prevalence ranging from 6 to 13 per 1000 live births.^{1,2} In the United Kingdom alone, there are ≈4600 babies born with CHD each year. Despite a constant decline in mortality rate, CHD still represents the primary cause of death among infants in industrialized countries. The definitive therapeutic option for these patients

is corrective surgery.³ However, prostheses currently used to reconstruct complex cardiac defects, including synthetic Gore-tex material, xenografts and homografts, are unable to match the growth of an infant's heart and they become dysfunctional over time.⁴ Consequently, CHD patients usually undergo repeated risky, distressing, and costly operations for replacement of failed grafts. The cost of reoperation on a

From the Divisions of Experimental Cardiovascular Medicine (E.A., I.R.A., H.L.S., F.R., G.M., S.C.S., J.R., V.V.A., O.O.I., S.S., A.O., P.M.), Cardiac Surgery (G.A.), and Congenital Heart Surgery (M.M.S., H.J., M.T.G., M.C.) and School of Physiology and Pharmacology (C.H.T.K., H.C., J.C.H., C.H.O.) and Vascular Pathology and Regeneration (C.E.), Bristol Heart Institute, University of Bristol, United Kingdom; Imperial College of London, United Kingdom (G.A., C.E.).

Accompanying Figures S1 through S4 are available at <http://jaha.ahajournals.org/content/4/6/e002043/suppl/DC1>

*Dr Avolio, Mr Rodriguez-Arabaolaza, and Dr Spencer contributed equally to the work.

Correspondence to: Paolo Madeddu, MD, Experimental Cardiovascular Medicine Division, Bristol Heart Institute, University of Bristol, Bristol Royal Infirmary—Level 7, Upper Maudlin St, BS2 8HW Bristol, United Kingdom. E-mail: mdprm@bristol.ac.uk and Massimo Caputo, MD, Division of Congenital Heart Surgery, Bristol Heart Institute, University of Bristol, Bristol Royal Infirmary—Level 7, Upper Maudlin St, BS2 8HW Bristol, United Kingdom. E-mail: Massimo.Caputo@bristol.ac.uk
Received March 31, 2015; accepted May 22, 2015.

© 2015 The Authors. Published on behalf of the American Heart Association, Inc., by Wiley Blackwell. This is an open access article under the terms of the Creative Commons Attribution-NonCommercial License, which permits use, distribution and reproduction in any medium, provided the original work is properly cited and is not used for commercial purposes.

healthcare budget is substantial. In the United States, the direct healthcare expenditure for every 100 cases undergoing cardiac reoperation is over \$2.4 million.

Cell therapy and tissue engineering hold promises for the repair of injuries to, or congenital defects of complex organs including the heart.^{5,6} The underlying concept is that incorporation of cells shall confer prosthetic grafts with the characteristics of a living tissue that grows and remodels in a physiologic manner in parallel with cardiac and whole-body growth.^{7,8} Initial preclinical and clinical studies focused on the implantation of valve leaflets seeded with vein-derived autologous endothelial cells (ECs),⁹ or peripheral blood-derived endothelial progenitor cells.^{10,11} However, for complex cardiac defects, such as tetralogy of Fallot, which require both valve replacement and ventricular reconstruction, a spectrum of cells able to reconstitute all the components of the heart should be considered. Multipotent stem cells (SCs) offer the all-in-one solution, whereas lineage-committed progenitor cells represent a safer option.

Pericytes are attracting attention for use in regenerative medicine and tissue engineering approaches.¹² In the heart, pericytes act as an interface between the coronary vasculature and cardiomyocyte compartment, playing an important role in maintenance of cardiac homeostasis and repair.¹³ Whether pericytes represent a homogeneous population remains a matter of debate. A recent study reported that immunosorted CD146^{pos}/CD34^{neg} perivascular cells from fetal and adult myocardium share certain phenotypic and developmental similarities with skeletal muscle pericytes, yet exhibit different antigenic, myogenic, and angiogenic properties, thus suggesting the heterogeneity of pericytes derived from diverse anatomical locations.¹⁴ Additionally, a different pericyte subtype expressing the transmembrane glycoproteins CD34 and CD105 together with stemness markers, but negative for CD146 as well as vasculogenic (α -smooth-muscle actin), hematopoietic (CD45), and endothelial (CD31) markers, has been described by us and others in the adventitia of large vessels.^{15–18} Our group was the first to identify that the adventitia of human fetal aorta contains CD34^{pos} progenitor cells capable of inducing vasculogenesis, angiogenesis, and myogenesis¹⁵ and starting from this discovery has then moved to appreciate the presence of CD34^{pos} pericyte progenitors in adult saphenous vein leftover material from coronary artery bypass graft surgery.¹⁶ Importantly, we have shown that, in models of peripheral and myocardial ischemia, transplantation of adventitial pericytes stimulates tissue repair both directly, acting as vascular progenitor cells, and indirectly, promoting the formation/maturation of new vessels, attracting pro-angiogenic monocytes and resident cardiac SCs (CSCs) and inhibiting cardiac fibrosis.^{15,16,19}

Comparing fetal and adult pericytes, we have also appreciated the higher plasticity of those derived from the youngest

donors.^{15,16} This prompted us to hypothesize that leftover material from pediatric cardiac surgery might represent a rich source of cells to be applied in regenerative medicine approaches. Since this has not been studied so far, we have embarked on this program of research. Hence, the present study aimed to verify whether cells similar to adventitial pericytes exist in human hearts. Using a standard operating procedure previously set up to obtain pericytes from surplus of human veins, we have been able to isolate and expand millions of pericytes from small cardiac leftovers obtained during CHD surgery. We found that these cardiac pericytes (CPs) are able to differentiate into vascular smooth muscle cells (VSMCs), attract ECs and CSCs, produce extracellular matrix proteins, and colonize a decellularized xenograft routinely used in cardiac surgery. Pericytes expanded from small leftovers of palliative surgery may represent a new therapeutic cell product for tissue engineering-based correction of CHD.

Methods

Ethics

Clinical characteristics of patients recruited to the study are shown in Table. Studies complied with the principles stated in the Declaration of Helsinki. The protocol for collection of cardiac leftovers from patients undergoing corrective surgery of CHD was approved by the North Somerset and South Bristol Research Ethics Committee (REC reference 11/SW/0122). The protocol for collection of saphenous veins samples was approved by Bath Research Ethics Committee (REC reference 06/Q2001/197). Adult patients and pediatric patients' custodians gave written informed consent for inclusion in the study.

Table. Clinical Characteristics of Patients With Successful Expansion of Cardiac Pericytes

Cell Line	Age	Source	Pathology
1	4 months	Atrium	Ventricular septal defect
2	6 months	Atrium	Ventricular septal defect
3	1 month	Atrium	Total anomalous pulmonary venous connection
4	2 months	Atrium	Hypoplastic left ventricle
5	6 months	Atrium	Tetralogy of Fallot
6	4 years	Atrium	Tetralogy of Fallot
7	6 months	Ventricle	Ventricular septal defect
8	6 months	Ventricle	Ventricular septal defect
9	6 months	Ventricle	Tetralogy of Fallot
10	17 months	Ventricle	Tetralogy of Fallot

Standard Operating Procedure for Pericyte Isolation and Expansion

We have applied a good manufacturing practices-compliant standard operating procedure previously employed for derivation of pericytes from human saphenous vein.¹⁶ CPs were isolated from atrium or ventricle specimens (3 to 5 mm, <100 mg) from infants and children undergoing surgical repair for congenital heart defects. In brief, discarded tissue was thoroughly washed in PBS and then manually minced. The tissue suspension was incubated for 40 minutes with 0.45 WU/mL/g Liberase 2 (Roche Technologies, UK). Passing the cell suspension sequentially through 70, 40, and 30- μ m cell strainers ensured single cell suspension. Cells were depleted for ECs with anti-CD31 conjugated beads (Miltenyi Biotec, UK), following the manufacturer's instructions. The remaining cells were purified by selecting CD34+ cells by anti-CD34 beads (Miltenyi Biotec). Target cells were cultured in the presence of EGM2 medium (Lonza, UK) supplemented with 2% fetal bovine serum (FBS). Adherent colonies were passaged to new culture dishes once they reached 60% to 70% confluence and frozen stocks were generated after Passage 2 for the experiments shown in this study. Trypsin-EDTA (Life Technologies, UK) was utilized to detach cells from the growth substrate.

Flow Cytometry Analysis

CPs were stained for surface antigen expression using combinations of the following antibodies to confirm typical phenotype at P5: anti-CD31 (eBioscience, UK), anti-CD34 (eBioscience), anti-CD44 (eBioscience, UK), anti-CD45 (Miltenyi Biotec), anti-CD90 (BD Biosciences, UK), anti-CD105 (Life Technologies), and anti-CD146 (Miltenyi Biotec). After staining, fluorescence was analyzed using a FACS Canto II flow cytometer and FACS Diva software (both BD Biosciences, UK).

Immunofluorescence Analysis

Cells at P5 were fixed with freshly prepared 4% (w/v) Paraformaldehyde for 20 minutes at room temperature, washed with PBS, and probed with the following antibodies: NG2 (1:100, Merck Millipore, UK), platelet-derived growth factor receptor- β (PDGFR- β) (1:50, Santa Cruz, UK), vimentin (1:100, Abcam, UK), GATA-4 (1:50, Santa Cruz), OCT-4 (1:400, Abcam, UK), SOX-2 (1:100, Merck Millipore), and c-Kit (1:40, DAKO, UK). For stemness markers, cells were used also at earlier (P3) and later (P9) passages. For VSMC characterization: α -smooth-muscle actin (1:100, DAKO), α -smoothelin (1:50, Abcam), α -Non-muscle Myosin IIB (1:500, Abcam), α -smooth muscle-myosin heavy chain 11 (1:50, Abcam), α -retinol-binding protein 1 (1:100, Abcam), and α -calponin (1:100, Abcam). For endothelial cell characterization: VE-Cadherin (1:50, Santa

Cruz), VEGFR-2 (1:50, Cell signaling, UK), and von Willebrand Factor (1:50, DAKO, UK). For cardiomyocyte cell characterization: α -sarcomeric Actinin (1:500, Sigma-Aldrich, UK) and Connexin 43 (1:40, Santa Cruz). For detection of intracellular antigens, cells were permeabilized for 10 minutes at room temperature with 0.1% (v/v) Triton X100 (Sigma-Aldrich) diluted in PBS. Primary antibodies were incubated for 16 hours at 4°C apart from c-KIT and Connexin 43, which were incubated for 2 hours at 37°C. Secondary antibodies were incubated on the cells for 1 hour at 20°C in the dark (1:200 anti-rabbit Alexa 488, 1:200 anti-mouse Alexa 488, or Alexa 568 [Life Technologies, UK]). The nuclei were counterstained with 4',6-diamidino-2-phenylindole (DAPI) (Sigma-Aldrich). Slides were mounted using *Fluoromount-G* (Sigma-Aldrich). Cells were analyzed at a \times 400 magnification. Adobe Photoshop software was utilized to compose and overlay the images (Adobe). All experiments were performed in triplicate with 3 to 7 cell lines assessed.

Immunohistochemical Analysis of Cardiac Tissue

Tissue sections 8 μ m thick were obtained from OCT (O.C.T. Compound, Tissue-Tek) embedded discarded cardiac tissue. Samples were snap-frozen and sections were fixed in -20°C acetone for 10 minutes. Tissues were permeabilized with 0.1% Triton-X (Sigma-Aldrich) for 10 minutes at 20°C. Sections were incubated for 16 hours with primary antibodies at 4°C. The primary antibodies that were used were as follows: 1:100 rabbit anti-human NG2 (Millipore, UK); 1:100 rabbit anti-human CD146 (Abcam), 1:200 sheep anti-human CD34 (DAKO); 1:100 rabbit anti-human PDGFR β (Insight Biotechnologies, UK); and 1:100 mouse anti-human CD31 (DAKO). Secondary antibodies were incubated on the cells for 1 hour at 20°C in the dark (1:200 goat-anti-mouse Alexa 547, 1:200 donkey-anti-sheep Alexa 488 (Life Technologies), and 1:200 goat-anti-rabbit Cy5 (Strattech Scientific, UK). The nuclei were counterstained with DAPI (Sigma-Aldrich). Slides mounted using *Fluoromount-G*.

CPs Growth Curve

Three CP lines were cultured in the microvascular medium EGM-2+2%FBS and 2 mesenchymal stromal cell media (STEM-MACS+10%FBS from Miltenyi Biotec, and DMEM+20%FBS from Life Technologies) to determine the optimal expansion medium for the cells. CPs (30 000) were seeded in each well of a 6-MW plate at day 1, and cells were detached and counted at day 4, 5, 6, 7, and 8 of culture.

Clonogenic Assay

To test the ability of CPs to generate colonies starting from a single cell, CPs (n=4) at P5 were selected as Propidium

Iodide negative (live cells) and sorted into single cells using a BD Bioscience Influx sorter (BD Biosciences, UK). Sorted cells were placed into each well of a 96-well culture plate (Greiner Bio-one, UK). The sorted cells were cultured up to 4 weeks in EGM-2 and the number of colonies generated was counted.

Multilineage Differentiation Toward the 3 Cardiovascular Lineages

The ability of CPs to differentiate into cardiomyocytes, ECs or VSMCs were tested following exposure to inductive media as previously described.^{16,20,21} Cells were seeded at 5000 cells/cm² and allowed to become confluent. The culture media exchange every 3 days, for 14 to 21 days. The following differentiation methods and media were used: (1) *Endothelial cell differentiation*: ECs were generated using either a previously described method—which provides the culture of cells in medium enriched with 10 ng/mL human VEGF (vascular endothelial growth factor, PeproTech EC Ltd, UK)—or CFU-Hill Liquid Medium Kit (StemCell Technologies, UK). (2) *Cardiomyocyte cell differentiation*: 2 different previously published methods were employed. The first is based on the culture of cells with a medium containing ascorbic acid (Sigma-Aldrich), 10 ng/mL human basic fibroblast growth factor, 10 ng/mL human VEGF, and 10 ng/mL human insulin-like growth factor 1 (all from PeproTech EC Ltd). The second method described in Smits et al, consists of an initial 3 day-long incubation of the cells with 5 μmol/L 5-aza-2'-deoxycytidine (Sigma-Aldrich) followed by the culture of cells with a medium containing ascorbic acid and 1 ng/mL human transforming growth factor β-1 (PeproTech EC Ltd). (3) *Vascular smooth muscle cell differentiation*: differentiation medium added with 20 ng/mL of human PDGF-BB (PeproTech). All the experiments were performed in triplicate with 2 to 4 cell lines assessed.

Analysis of CPs Cell Secretome by ELISA

The quantities of the following secreted proteins were determined in CPs cultured when cells were exposed to normoxic conditions for 48 hours in serum-free medium: human VEGF, basic fibroblast growth factor, hepatocyte growth factor, angiotensin-1, angiotensin-2, and stromal cells-derived factor 1, transforming growth factor-β1, and procollagen type I (all from R&D Systems, UK). ELISAs were performed following manufacturer's instructions. Cytokine concentrations were expressed normalizing the data for the number of the cells at the end of the collection time, and for the time of incubation. Four different CPs lines were assessed and experiments were performed in triplicate.

In Vitro Matrigel Assay

Network formation was performed as described previously.¹⁶ Briefly, CPs were labeled with VyBrant dil (Life Technologies) and seeded with human umbilical vein endothelial cells (HUVECs, Lonza, UK, 1:4 ratio of CPs to HUVECs, respectively) in a 96-well plate at 7000 cells/well on top of 70 μL thick-coated Matrigel (BD Biosciences) in EGM2 with FBS for 6 hours. HUVECs and CPs were also seeded alone as a control. To assess the effect of CP-secretome, CP-conditioned media diluted 1:2 with fresh EGM-2 and FBS were incubated with 7000 HUVECs/well on top of 70 μL thick-coated Matrigel for 6 hours. HUVECs with un-conditioned EGM-2 were also seeded alone as a control. FBS concentration was the same in all the experimental conditions. CPs-alone network formations were also assessed at different cell numbers (2000, 5000, 7000). Images were taken under bright-field at 5× and the length of the networks was measured. All experiments were performed in triplicate with 3 to 4 cell lines assessed.

Labeling of Cells With Dil Tracker

For selected in vitro experiments, CPs were stained with the long-term cell trackers VyBrant dil (Life Technologies). Dil was diluted 1:1000 in PBS and incubated with confluent cells (adherent to the culture plate) for 5 minutes at 37°C and then on ice for an additional 15 minutes, in the dark. Cells were then washed with PBS, left to recover for 24 hours, and used for experiments.

Transwell Migration Assay

To test the capacity of CPs secretome to induce the migration of human CSC and HUVECs, 60 000 CSC or HUVECs were seeded in 24-well plates on a 6.5-mm Transwell[®] with 5.0-μm pore polycarbonate membrane insert (Corning, UK), in serum-free EGM-2 medium (Lonza). In the bottom of the wells, 0.5 mL of CPs serum-free conditioned medium was added. Serum-free EGM-2 medium was used as negative control. Serum-free EGM-2 supplemented with human VEGFa (100 ng/mL; PeproTech EC Ltd) was used as a positive control for HUVECs. Cells were incubated for 16 hours at 37°C. At the end of this period, the membrane inserts were washed with PBS, fixed with ice-cold methanol for 15 minutes at room temperature, stained with DAPI, and mounted on a slide. Membranes were analyzed with an epifluorescence microscope at ×200 magnification; 10 fields were randomly acquired and cells counted. Migrated cells were expressed as a percentage. Experiments were performed in duplicate. Four different CPs lines were assessed.

Measurement of Membrane Current and Intracellular Ca²⁺

To measure membrane current, CPs were placed in an experimental chamber mounted on the stage of an inverted microscope, and superfused with solution containing (in mmol/L): 140 NaCl, 4 KCl, 2 CaCl₂, 1 MgCl₂, 10 glucose, 5 HEPES (pH 7.4 with NaOH) at 35 to 37°C. Membrane currents were monitored with the whole-cell patch-clamp technique, using an AxoPatch-1D amplifier (Axon Instruments, USA). The pipette solution contained (in mmol/L): 110 KCl, 10 NaCl, 10 HEPES, 0.4 MgCl₂, 5 glucose, 5 K₂ATP, 0.5 GTP-Tris, with or without 5 1,2-bis(o-aminophenoxy)ethane-N,N,N',N'-tetraacetic acid (pH 7.1 with KOH). Protocols were generated and data recorded using pClamp 10 software (Axon Instruments) via an A/D converter (Digidata 1440A, Axon Instruments/Molecular Devices, USA). Whole-cell membrane currents were recorded in voltage-clamp mode using either a ramp protocol, in which membrane potential was ramped from -120 mV to +80 mV over 400 ms from a holding potential of either -40 mV or -80 mV, or a step protocol, in which membrane potential was stepped between -120 mV and +80 mV in increments of 10 mV for 500 ms, from a holding potential of either -40 mV or -80 mV. Ramps and steps were applied at a frequency of 0.2 Hz. Data were filtered at 1 kHz and digitized at 10 kHz.

To measure intracellular Ca²⁺, CPs were incubated with 5 μmol/L Fluo-4/AM (Life Technologies) for 25 minutes at room temperature, before being rinsed in control solution. The cells were then placed in an experimental chamber mounted on the stage of either a Fluoview 1200 (Olympus, Germany) or Pascal (Zeiss, Germany) inverted confocal microscope, and superfused with control solution at room temperature. Fluo-4 fluorescence was stimulated at 488 nm. Fluorescence was normalized to F/F₀ as described previously, following correction for photobleaching.²² Cells were stimulated either electrically, via parallel Pt wires connected to an SD8 Grass Stimulator, or using 10 μmol/L BT₃-IP₃/AM (a membrane-permeable form of IP₃) or 10 mmol/L caffeine added to the superfusate.

Assays on Gene Expression

RNA isolation and quantitative real time (RT) polymerase chain reaction (PCR)

Extracted total RNA was reverse-transcribed into single-stranded cDNA using a High Capacity RNA-to-cDNA Kit (Life Technologies) or using specific primers provided with the Taqman miRNA assay and microRNA Reverse Transcription Kit (Life Technologies). The reverse transcription-PCR was performed using first-strand cDNA with TaqMan Fast Universal PCR Master Mix (Life Technologies). Quantitative PCR was

performed on a LightCycler480 Real-Time PCR system (Roche Technologies, UK). Quantitative PCR parameters for cycling were as follows: 50°C incubation for 2 minutes, 95°C for 10 minutes, 40 cycles of PCR at 95°C for 15 seconds, and 60°C for 1 minute. The following Taqman assays were used: UBC (Hs00824723_m1) as a housekeeper, *for smooth muscle differentiation characterization*: calponin 1 (Hs00154543_m1); smooth muscle-myosin heavy chain (Hs00224610_m1); retinol-binding protein 1 (Hs01011512_g1); smooth muscle actin (Hs00426835_g1), smoothelin (Hs00199489_m1); *for endothelial differentiation characterization*: KDR (Hs00911700_m1); CD31 (Hs00169777_m1); von Willebrand Factor (Hs01109446_m1); *for cardiomyocytes differentiation characterization*: Brachyury (Hs00610080_m1); Connexin 43 (Hs00748445_s1); NKX2.5 (Hs00231763_m1); MYH7 (Hs01116032_m1); ISLET1 (Hs00158126_m1); CACNAC1 (Hs00167681_m1), Tbx5 (Hs03675785_s1). All reactions were performed in a 10-μL reaction volume in triplicate. The mRNA expression level was determined using the 2^{-ΔCt} method. Each reaction was performed in triplicate.

Static Culture of Cardiac Pericytes on the CorMatrix

Pieces of CorMatrix[®] ECM[®] (CorMatrix Cardiovascular, Sunnyvale, CA) — a decellularized xenograft material clinically approved for use in cardiac surgery — of ≈1.5-cm diameter were cut and placed in wells of a 24-well plate. To fix the bioscaffold pieces to the bottom of the wells, CellCrown inserts were used (Sigma-Aldrich). Prior to the seeding, the bioscaffolds were incubated for 2 days with EGM-2 media. CPs (50 000) at P5 were seeded into each CorMatrix-containing well and maintained for 7 days on the bioscaffolds. The bioscaffolds were fixed in 4% Paraformaldehyde for 20 hours at 4°C and imbedded in paraffin or OCT-frozen. Eight-micrometer sections were examined for the presence of CPs using anti-vimentin, NG2, and PDGFR-β antibodies (see above), which were incubated for 20 hours at 4°C after permeabilization and blocking. Secondary antibody was incubated on the sections for 1 hour at room temperature. The nuclei were counterstained with DAPI (Sigma-Aldrich). The slides were mounted using Fluoromount-G[®] mounting media (Sigma-Aldrich) and immunofluorescence pictures were taken after 24 hours both at ×20 and ×40.

Dynamic Culture of CPs on CorMatrix

Pericytes were seeded onto the CorMatrix scaffold (CorMatrix Cardiovascular) at 0.5 million cells/cm² and cultured for 1 week under static conditions followed by 2 weeks under dynamic conditions. For the dynamic cell culture, the pericyte-

seeded CorMatrix was grown in an InBreath Bioreactor (Harvard Apparatus, Holliston, MA). The device ensures maintenance of sterility and stabilization, automation, and scale-up/-out of the cellularization process through hydrodynamic stimuli and control of nutrients and oxygen transport to the cells. The conduit was stitched to the rotating arm of the Bioreactor and stitched back onto itself so as to fashion a tube shape through the center of which runs the rotating arm. The Bioreactor was filled with EGM-2 medium and placed into the incubator at 37°C with the medium being changed twice a week. At the end of the total 3 weeks of culture, the viability of the seeded cells on the scaffolds was detected using the Biotium fluorescent viability/cytotoxicity Assay kit. Fluorescence imaging was carried out on the whole thickness of graft. Tissue-engineered scaffolds were then analyzed by histological staining of the nuclei and of the extracellular matrix components elastin and collagen, detected, respectively, by hematoxylin and eosin (H&E) and Elastic Van Gieson staining.

Statistical Analysis

GraphPad Prism was used to perform the statistical analysis. Due to the limited number of samples ($n=3$ to 4, too small), a normality test could not be performed. For this reason, 2-group analysis was performed by nonparametric Mann–Whitney test. Values were expressed as means \pm standard error of the mean (SEM). Probability values (P) <0.05 were considered significant.

Results

Immunohistochemical Localization of CPs

Multiple staining immunohistochemistry and confocal microscopy were used for cell localization in cardiac tissue (Figure 1). CD31^{pos}/CD34^{pos} ECs were typically recognized around the lumen of capillaries and arterioles. Moreover, we identified CD31^{neg}/CD34^{pos}/NG2^{pos} cells around capillary ECs (Figure 1A) and especially within the layer external to NG2^{pos} VSMCs in arterioles (Figure 1B). Additionally, CD31^{neg}/CD34^{pos} CPs do not express CD146 (Figure 1C).

Isolation/Expansion and Characterization of CPs

The good manufacturing practices-compliant standard operating procedure, previously employed for derivation of saphenous vein pericytes,¹⁶ proved to be highly efficient when applied to cardiac leftovers, with an expansion success (≈ 20 million cells at P5, in 4 to 6 weeks) of 10 samples out of 13 examined. This is a remarkable result, considering the weight of source cardiac tissue in comparison with saphenous veins (Figure S1). CPs can

be successfully expanded in EGM-2 supplemented with 2% FBS (both from Lonza), a microvascular media that we already use for optimal expansion of saphenous vein pericytes. The attempt to culture CPs in 2 mesenchymal stromal cell media (STEM-MACS+10%FBS from Miltenyi Biotec, and DMEM+20%FBS from Life Technologies) clearly showed that EGM-2 is the optimal medium for expansion of CPs (Figure S2).

With use of contrast phase microscopy, expanded cells show typical spindle-shape morphology (Figure 2A). Cells at P5 ($n=8$ donors) were assayed for their antigen expression by flow cytometry and immunocytochemistry, which showed superimposable characteristics of atrium- and ventricle-derived cells. Flow-cytometry analysis of expanded cells indicates high abundance of CD44 and CD105 and variable expression of CD90 (Figure 2B). In contrast, there was a scarcity/absence of endothelial-CD31 and hematopoietic-CD45 markers. Another unique characteristic is the lack of CD146, which distinguishes the isolated population from CD146^{pos} pericytes described previously in postmortem samples from fetal and adult hearts.¹⁴ Moreover, as shown by us with saphenous vein-derived pericytes, expansion in culture was associated with an expected downregulation of CD34. Immunocytochemical analyses showed the consistent expression of vimentin (100%), NG2 (95%), and PDGFR β (58%). Additionally, expanded cells were positive for the cardiac transcription factor GATA-4 (47%) and for the stemness markers OCT-4 (64%), SOX-2 (54%), and NANOG (34%) (Figure 3A). Around 30% of the total population showed coexpression of OCT4/NANOG and SOX-2/NANOG (Figure 3B). The expression of stemness markers slightly decreased along with cell expansion, from passage 3 to passage 5 of culture (OCT-4 58%, SOX-2 50%, NANOG 28%), but the difference was not significant (Mann–Whitney test, OCT-4 $P=0.72$, SOX-2 $P=0.23$, NANOG $P=0.63$) (Figure 3C). As expected, a further decreasing trend was observed up to passage 9 (OCT-4 39% and NANOG 14%, Mann–Whitney test P3 versus P9: OCT-4 $P=0.4$, NANOG $P=0.1$). Finally, CPs did not express the mast/stem cell growth factor receptor (SCFR/c-Kit), indicating their distinction from classical cardiac stem cells currently used in clinical trials^{23,24}.

We next assessed the ability of CPs ($n=4$ donors) to secrete growth factors, cytokines, and extracellular matrix protein (Figure 4). We found that hepatocyte growth factor was the most abundant secreted factor, followed by angiopoietin 2, VEGF-A, angiopoietin 1, stromal cell derived factor-1 α , and fibroblast growth factor-B. Furthermore, we found that CPs release procollagen type 1, a major constituent of cardiac extracellular matrix, in conditioned media (0.8 ± 0.1 ng/mL, $n=4$ lines). Instead, CPs do not release transforming growth factor- β 1 in the culture media. Comparison with saphenous vein-derived pericytes indicates

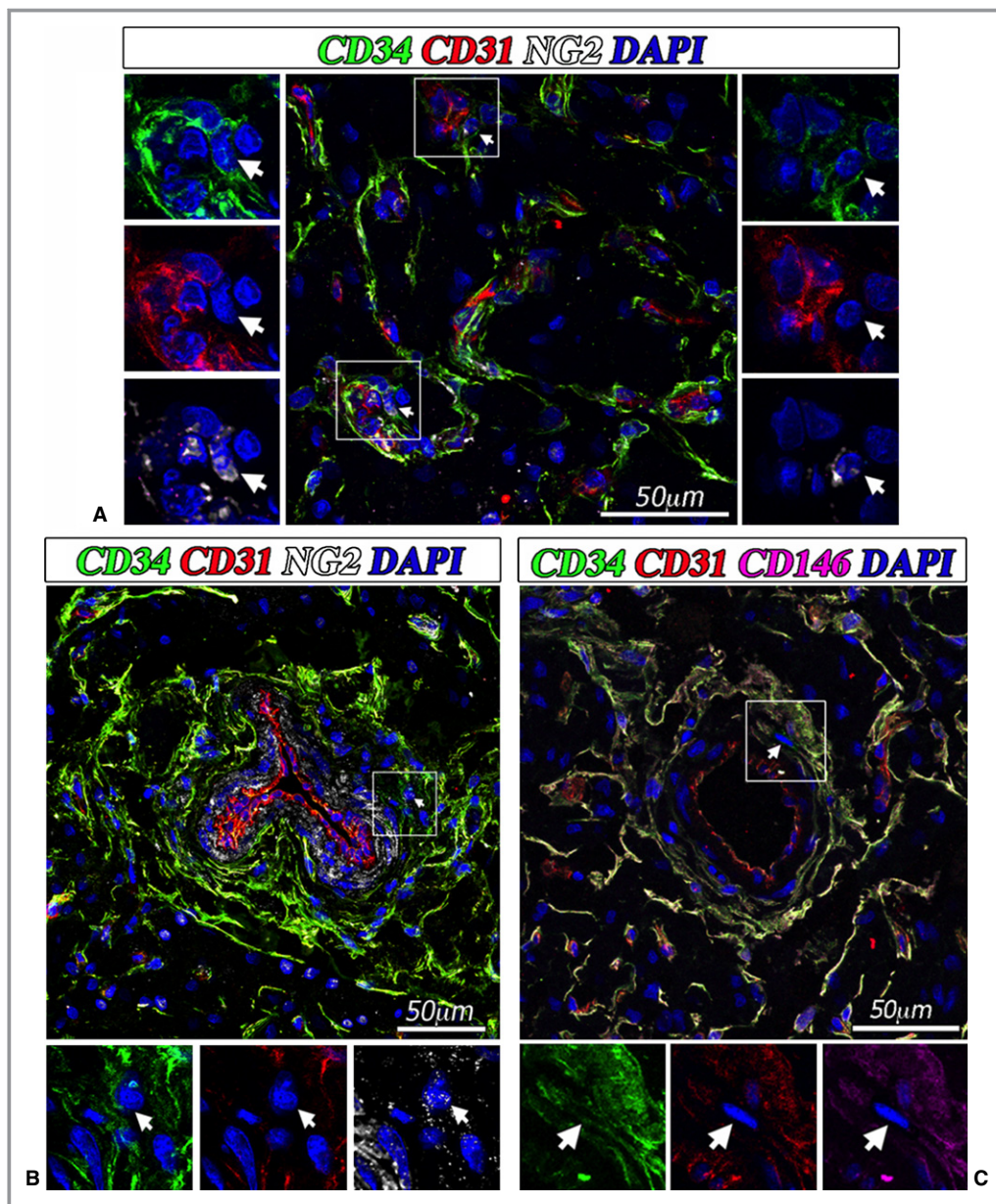


Figure 1. Localization of cardiac pericytes in situ. Confocal immunofluorescent images showing the perivascular localization of $CD31^{neg}/CD34^{pos}/NG2^{pos}/CD146^{neg}$ CPs in the neonatal human heart. CD34 is labeled in green fluorescence and CD31 in red, NG2 is depicted in white, CD146 is depicted in purple, and nuclei are recognized by the blue fluorescence of DAPI. In (A), the white arrows indicate 2 CPs around small vessels in association with $CD31^{pos}$ ECs. In (B) the white arrow indicates a $CD31^{neg}/CD34^{pos}/NG2^{pos}$ pericyte around an artery. The lumen of the artery is identified by a layer of $CD31^{pos}$ ECs, while the smooth muscle cells within the tunica media can be recognized by the positivity to NG2. In (C) the white arrow indicates a $CD31^{neg}/CD34^{pos}/CD146^{neg}$ pericyte around an artery. CPs indicates cardiac pericytes; DAPI, 4',6-diamidino-2-phenylindole; ECs, endothelial cells; NG2, neural/glia antigen 2.

similarity of the 2 cell populations, though CPs are more abundant in NG2 and express a spectrum of SC-associated antigens (Figure S3A). Moreover, CPs secrete more hepatocyte growth factor (6-fold), angiopoietin 2 (8-fold), FGF (4-fold), and VEGF (6-fold) than saphenous vein-derived pericytes (Figure S3B).

Clonogenic and Differentiation Potential

To investigate whether CPs are able to form clones, we seeded them (P5, from 4 donors) into 96-well Terasaki plates (1 cell per well). One week after sorting, we observed the formation of first colonies that contained 5

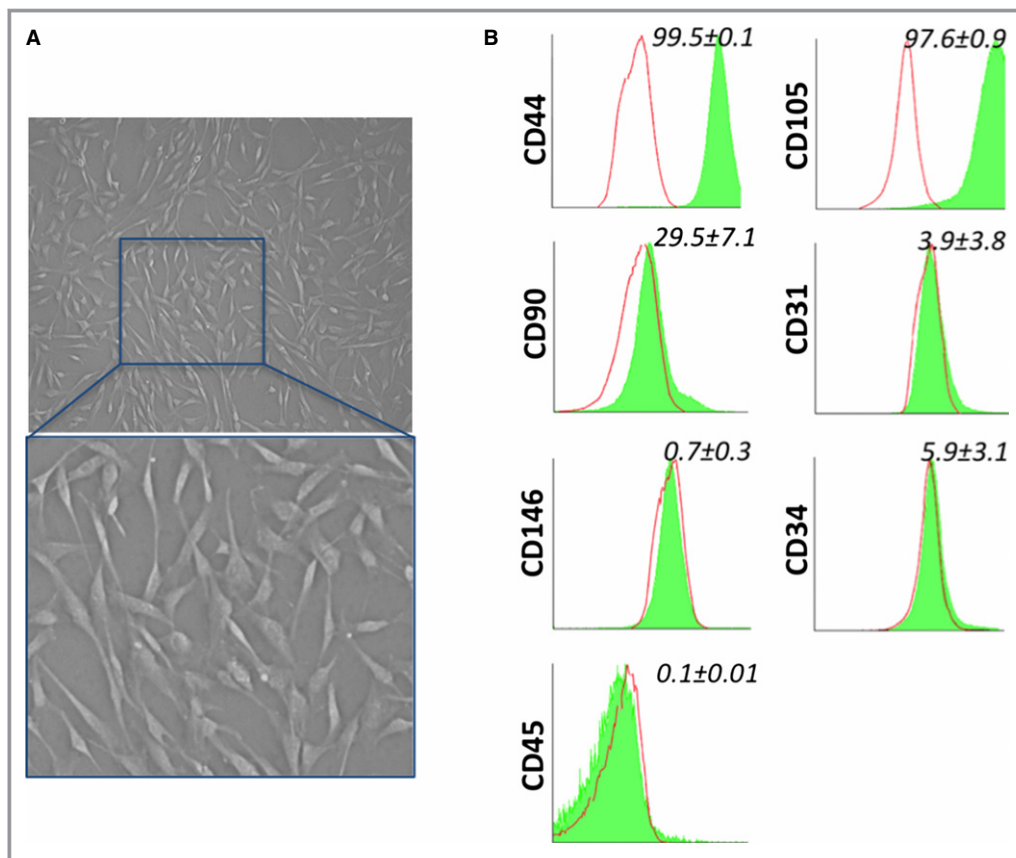


Figure 2. In vitro characterization of cardiac pericytes (CPs). (A) Representative phase-contrast optical image of CPs in culture (in the upper image magnification is $\times 200$). (B) Representative flow cytometry histograms of cultured CPs at P5. Isotype control IgG staining profiles are shown by the red border line histograms, while specific antibody staining profiles are shown by full green histograms. Data are expressed as means \pm SEM ($n=8$ CPs).

to 20 cells. At 4 weeks, we found that CPs from atrium or ventricle give rise to similar numbers of clones (10% and 11% of seeded cells, respectively), a result that surpasses the reported clonogenic activity of saphenous vein-derived pericytes (7%).¹⁶

We next exposed CPs ($n=4$ donors) to differentiation stimuli for derivation of vascular and cardiac lineages. As shown in Figure 5A, CPs do not express typical VSMC antigens. Following exposure to a differentiation medium enriched with human platelet-derived growth factor BB (PDGFBB),²⁵ they initially acquired the expression of nonmuscle myosin B, which is typical of synthetic VSMCs, and then additionally expressed retinol-binding protein 1, α -smooth-muscle actin, and smooth muscle-calponin, suggesting their maturation into a contractile phenotype. The analysis of gene expression by quantitative real time-PCR (Figure 5B) confirmed a marked induction of α -smooth-muscle actin (average 18-fold increase after 14 days) and SM-calponin (157-fold), while typical antigens of mature contractile VSMCs were less upregulated (smooth muscle-myosin heavy chain, average 5.5-fold increase after 14 days, and smoothelin, 4.2-fold

increase). In addition, retinol-binding protein 1 mRNA levels peaked at 7 days (3.1-fold) and returned to basal level at 14 days.

Culture of CPs in CFU-Hill Medium or a medium enriched with human VEGF-A failed to induce the expression of mature endothelial proteins as detected by immunocytochemistry (KDR/VEGFR2, von Willebrand Factor, VE-Cadherin) (data not shown); quantitative PCR analysis confirmed only a slight increase of von Willebrand Factor (2.5-fold), while CD31 and KDR were not increased or even downregulated (5-fold decrease), respectively, after the differentiation protocol compared to baseline CPs (Figure 5B).

To induce the differentiation into cardiomyocytes, we adopted 2 protocols that differ from each other in terms of growth factor composition and presence or absence of the epigenetic modifier 5-Azacytidine.^{20,21} We observed that CPs acquire the expression of α -Sarc-actinin and connexin-43, but do not show the localized pattern typically seen in mature cardiomyocytes (Figure 5C). Furthermore, quantitative real time-PCR analyses (Figure 5B) confirmed the induction of connexin-43 (average 9-fold increase after 21 days), T-box

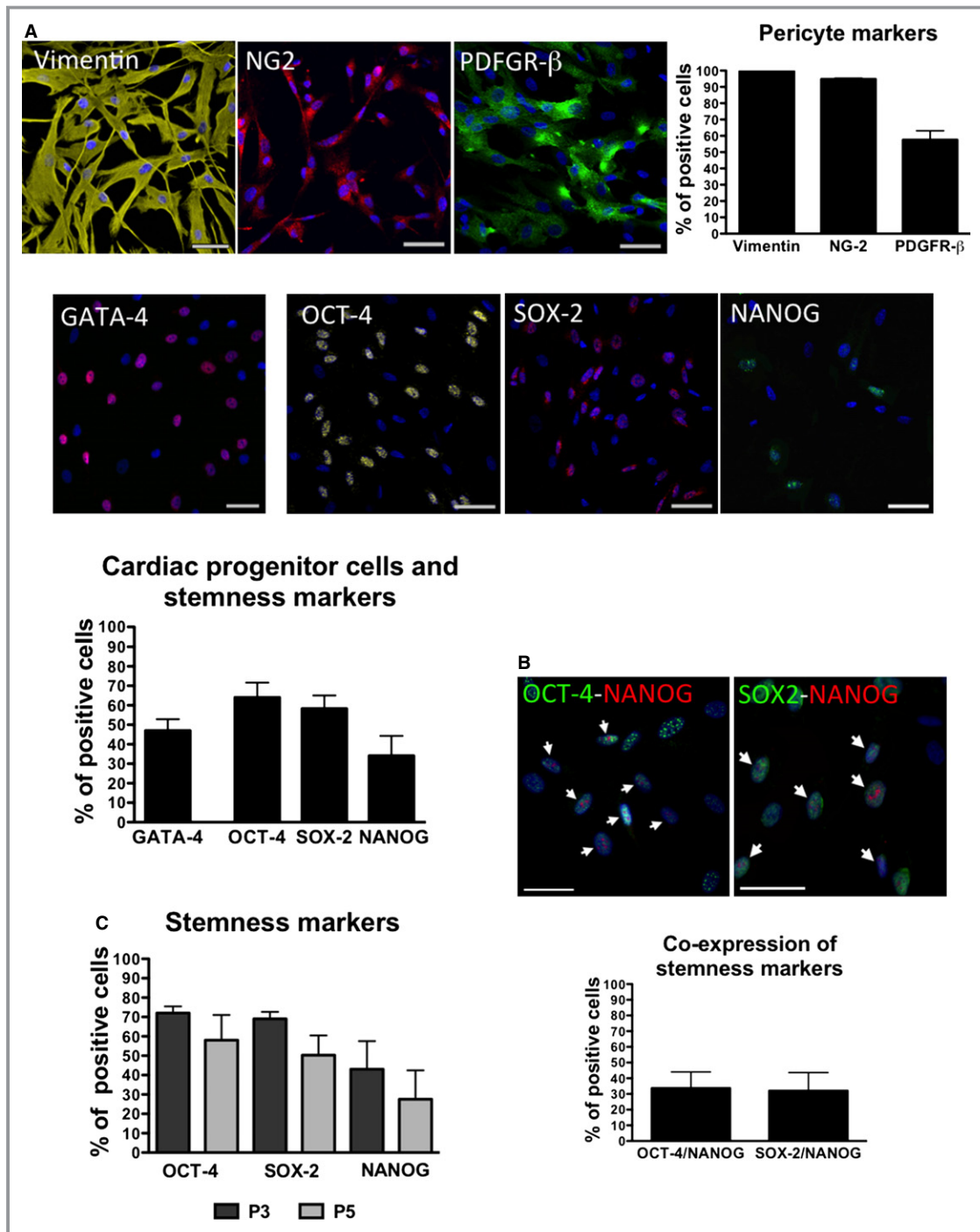


Figure 3. Immunofluorescence characterization of CPs. (A) Epifluorescence microscopy analysis of CPs at P5 for the expression of the pericyte markers vimentin, NG2, and PDGFR-β, the cardiac transcriptional factor GATA binding protein 4 (GATA-4) and the stemness markers octamer-binding transcription factor 4 (OCT-4), (sex determining region Y)-box 2 (SOX-2), and homeobox NANOG (NANOG). Nuclei are shown by the blue fluorescence of DAPI. Scale bar: 50 μm. Bar graphs show the percentage of cells positive for each marker. Data are expressed as means±SEM (n=4 CPs. Only for stemness markers, n=7). (B) Analysis of coexpression of stemness markers in n=3 lines of CPs, at passage 3 of culture. White arrows in the immunofluorescence microscopy pictures identify CPs coexpressing the indicated stemness markers; scale bar: 50 μm. In the bar graph, cells coexpressing the stemness markers are indicated as the percent of the entire population of cells. (C) Graph showing the expression of stemness markers in CPs at passages 3 and 5 of culture. Values are plotted as means±SEM, n=3. Values were not significantly different between P3 and P5 (Mann–Whitney test, OCT-4 *P*=0.72, SOX-2 *P*=0.23, NANOG *P*=0.63). CPs indicates cardiac pericytes; DAPI, 4',6-diamidino-2-phenylindole; NG2, neural/glial antigen 2; PDGFR-β, platelet-derived growth factor receptor-β.

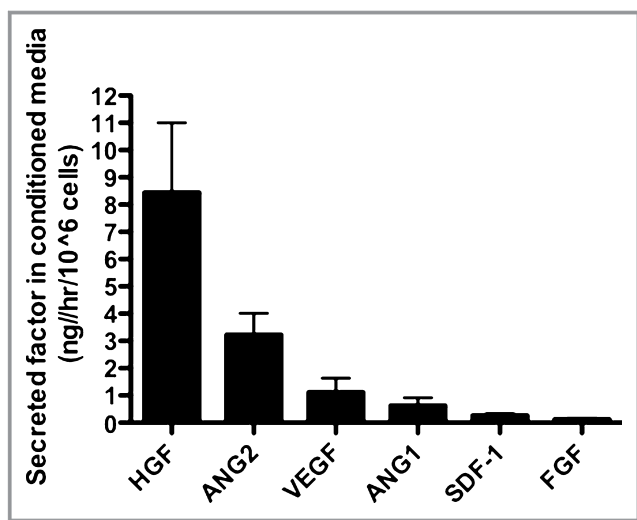


Figure 4. CPs secrete. Histograms show the amount of secreted factors in CP-conditioned media, normalized for the volume of the collected supernatant, cell number, and time of incubation. Data are expressed as means \pm SEM ($n=4$ CPs). ANG1 indicates angiotensin-1; ANG2, angiotensin-2; CPs, cardiac pericytes; FGF, fibroblast growth factor; HGF, hepatocyte growth factor; SDF-1, stromal cells-derived factor 1; VEGF, vascular endothelial growth factor.

transcription factor (Tbx5, a marker of cardiac development, 1.5-fold), and calcium channel, voltage-dependent, L type, α 1C subunit (CNAC1C, average 18-fold). However, the mesoderm marker brachyury, early cardiac markers Islet-1, and NK2 homeobox 5 (NKX2.5) as well as myosin heavy chain 7, cardiac muscle, β (MYH7) could not be detected. Failure of CPs to acquire typical cardiac transcription factors may indicate the incapacity to transverse the whole differentiation process.

To further verify the cardiomyogenic potential of CPs, we next assessed their electrical properties before and after induction of differentiation. Figure 6 shows examples of membrane current (Figure 6A) and intracellular Ca^{2+} (Figure 6B) measured from representative undifferentiated (left) and differentiated (right) CPs. In undifferentiated cells, depolarization of the cell membrane resulted in an outwardly rectifying membrane current, but did not activate voltage-dependent Na^+ or Ca^{2+} currents ($n=3$); these currents were also absent during step depolarizations ($n=2$). Membrane current was similar when holding potential was -80 mV or -40 mV (which would inactivate Na^+ current), and in the absence and presence of the intracellular Ca^{2+} chelator 1,2-bis(o-aminophenoxy)ethane-N,N,N',N'-tetraacetic acid. Na^+ and Ca^{2+} currents normally occur in electrically excitable cells, so these data suggest that the CPs are not electrically excitable and do not exhibit currents that are regulated by intracellular Ca^{2+} . They do, however, appear to have mechanisms for ion flux across the

cell membrane. Consistent with these data, electrical stimulation did not cause a rise of intracellular Ca^{2+} ($n=9$; not shown), although the cells possess releasable stores of intracellular Ca^{2+} , indicated by a transient increase of Ca^{2+} followed by a sustained rise during application of $\text{BT}_3\text{-IP}_3/\text{AM}$ ($n=5$ out of 5), as shown in the left panels of Figure 6B. The right panels show that cellular electrophysiology appeared unchanged following cardiomyocyte differentiation. However, there appeared to be no increase in intracellular Ca^{2+} in response to $\text{BT}_3\text{-IP}_3/\text{AM}$ ($n=6$ out of 6 cells). Similarly caffeine, which causes Ca^{2+} release from intracellular stores via ryanodine receptors, had no effect on intracellular Ca^{2+} ($n=5$ out of 5 cells). As a positive control, 110 mmol/L CaCl_2 was added to the perfusate, which resulted in an increase in intracellular Ca^{2+} in 3 out of 4 cells (insert in lower right panel of Figure 6B).

Interaction of CPs With ECs and CSCs

Recruitment of cardiac cells into the graft is important for its functionalization. CPs may help this process by releasing chemoattractant factors. In line with this possibility, results illustrated in Figure 7A and 7B indicate that the conditioned medium of CPs exerts strong attractive actions on c-kit^{pos} CSCs and ECs in an in vitro migration assay (8-fold increase in CSC and 15-fold increase in ECs migration as compared to unconditioned media; both $n=4$ donors, Mann-Whitney test, $P<0.03$). In addition, CPs are able to form networks in Matrigel in a dose-related fashion (Figure S4) and to enhance the network forming activity of ECs depending on the direct contact between the 2 cell types (2-fold; $n=3$, Mann-Whitney, $P<0.05$) (Figure 7C and 7D). These data confirm our previous findings of cooperative interactions between adventitial pericytes and ECs instrumental to promotion of vascular growth and stabilization.¹⁶ Instead, the proangiogenic effect was not observed when ECs were incubated with CP-conditioned media (Figure 7E). However, cautiousness is necessary when excluding a paracrine action of CPs in the observed phenomena, as direct contacts are often necessary to deliver chemical signals between cells. Furthermore, we have recently shown that cells in coculture influence the paracrine activity of each other.²⁶

Successful Seeding in Clinical-Grade Grafts

Finally, we seeded CPs (50×10^3 or 50×10^4 cells/cm²) on CorMatrix, a clinically approved xenograft material, and cultured them for 1 week under static conditions. In additional experiments, at the end of the 1-week static culture, the pericyte-engineered graft was transferred to a double-chamber rotating bioreactor, for an additional 2 weeks. Successful cellularization of the graft texture was demonstrated with histological stainings for cell nuclei and cytoplasm (hematox-

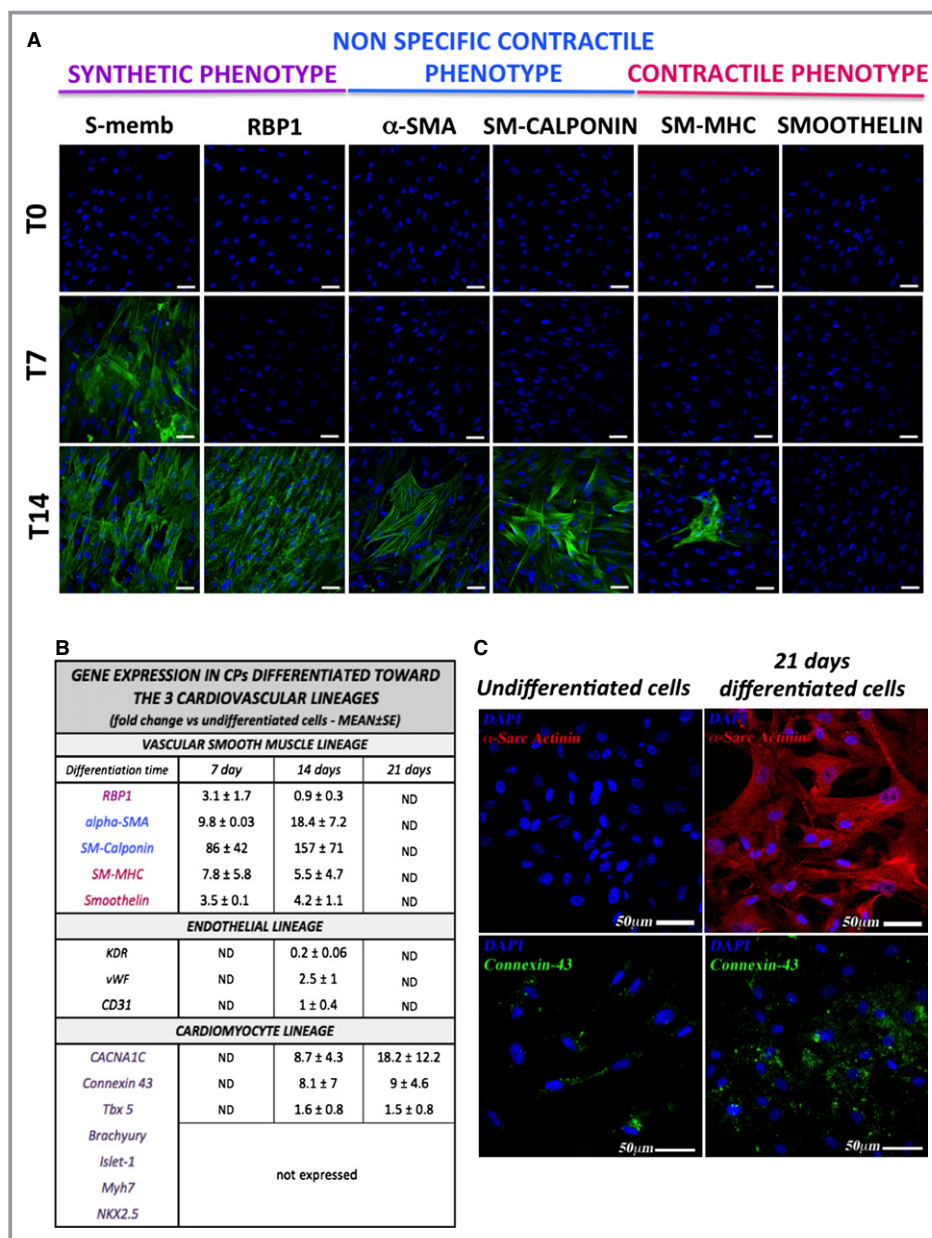


Figure 5. Differentiation of CPs toward the cardiovascular lineage. (A) At immunofluorescence analysis, undifferentiated CPs are negative for characteristic VSMC markers. After culture for 14 days with an inductive medium, cells express markers typical of the synthetic and early contractile phenotype (n=4 CPs). The VSMC markers are identified by green fluorescence; nuclei are shown by the blue fluorescence of DAPI. T0 indicates the time at which the differentiation has been started, T7 and T14 indicate the differentiation time (in days) from T0. Scale bar: 50 μm. (B) The table shows the expression of endothelial, vascular smooth muscle, and cardiomyocyte genes in CPs cultured for up to 21 days with inductive media. Numbers indicate the average fold change in gene expression compared to the basal undifferentiated CPs. Data are represented as means±SEM. (C) Immunofluorescence analysis of cardiomyocyte markers showing expression of α-Sarc Actinin (in red fluorescence) and Connexin-43 (in green). In blue, DAPI. For differentiation protocols, see Methods. n=2 CPs for endothelial and smooth muscle, n=3 for cardiac differentiation. CACNA1C indicates Calcium channel, voltage-dependent, L type, alpha 1C subunit; CPs, cardiac pericytes; DAPI, 4',6-diamidino-2-phenylindole; KDR/VEGFR2, vascular endothelial growth factor receptor 2; Myh7, myosin heavy chain 7, cardiac muscle, β; ND, not determined; NKX2.5, NK2 homeobox 5; RBP1, retinol binding protein 1; SM-MHC, smooth muscle–myosin heavy chain; VSMC, vascular smooth muscle cell; α-SMA, α-smooth muscle actin; Tbx5, T-box transcription factor; vWF, von Willebrand Factor.

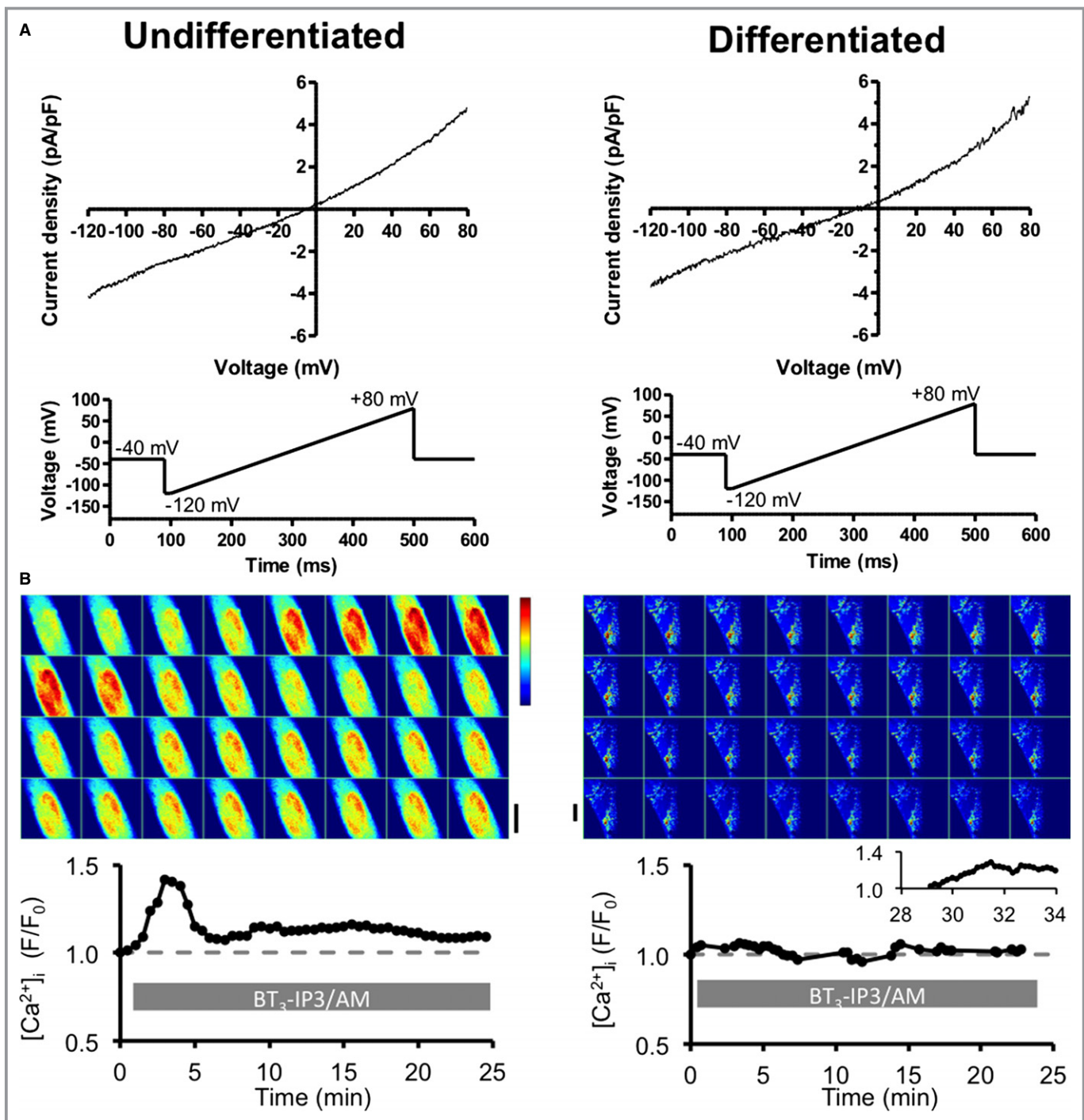


Figure 6. Electrophysiology study in cardiac pericytes (CPs) before and after differentiation toward the cardiomyocyte lineage. (A) Membrane current recorded from representative undifferentiated (left) and differentiated (right) CPs, during a depolarizing voltage ramp from -120 to $+80$ mV over 400 ms (shown below). (B) A time-series of confocal images of intracellular Ca²⁺, monitored using the Ca²⁺-sensitive fluorescent indicator Fluo-4, from representative undifferentiated (left) and differentiated (right) CPs during application of a membrane-permeable form of IP₃ to release Ca from intracellular stores. The rise in intracellular Ca²⁺ is denoted by the color shift from light blue toward red (shown in scale bar). The vertical scale bars indicate 20 μ m. Normalized Fluo-4 fluorescence is plotted against time in the bottom panels, where the presence of BT₃-IP₃/AM is indicated by the gray bar; the time-point for each image is indicated by a filled circle. The inset in the right panel shows the increase of intracellular Ca²⁺ following addition of 110 mmol/L CaCl₂ to the extracellular solution.

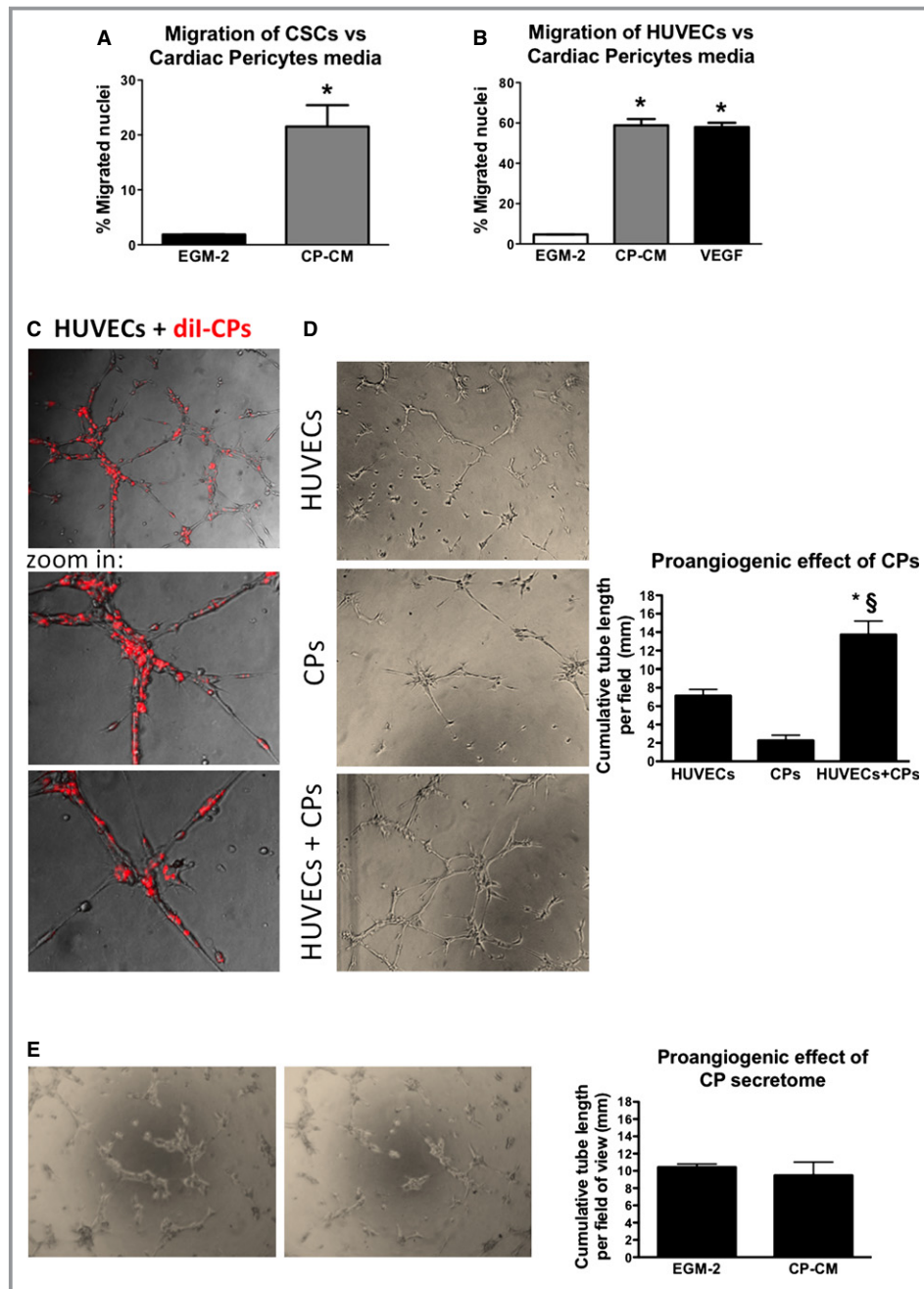


Figure 7. CPs recruit ECs and CSCs and support network formation by HUVECs. A and B, In multitranswell migration assay CP-CM showed the ability to enhance migration of CSCs (A) and HUVECs (B) (VEGF 100 ng/mL was used as positive control). Data are represented as means \pm SEM. * P <0.03 vs EGM-2. C and D, Representative phase-contrast and fluorescent images of HUVECs, CPs, and HUVECs+CPs in 4:1 ratio forming tubular networks when cultured for 6 hours on Matrigel substrate. In (C) CPs were labeled with the long-term cell tracker Dil (in red fluorescence) in order to investigate their ability to cooperate with HUVECs during the formation of tubular structures. Images have been acquired using a $\times 200$ magnification. Histograms summarize quantitative data of the tube length per field. Data are represented as means \pm SEM. $n=3$ per each group. * P <0.04 vs HUVECs, § P <0.05 vs CPs. E, Representative phase-contrast images of HUVECs incubated with CP-CM or EGM-2 for 6 hours on Matrigel substrate. Magnification $\times 50$. Histograms summarize quantitative data of the tube length per field. Data are represented as means \pm SEM. $n=4$ per each group. CP-CM indicates cardiac pericytes conditioned medium; CPs, cardiac pericytes; CSCs, cardiac stem cells; ECs, endothelial cells; EGM-2, endothelial growth medium 2; HUVECs, human umbilical vascular endothelial cells; VEGF, vascular endothelial growth factor.

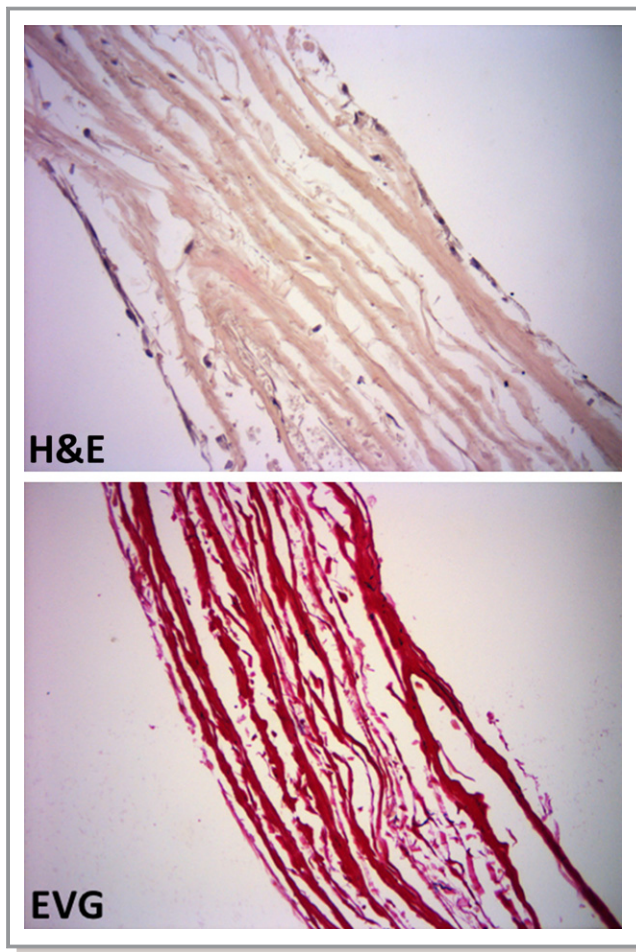


Figure 8. Analysis of CPs-engineered scaffold. Scaffolds were analyzed by histological staining of the nuclei and of the extracellular matrix components elastin and collagen, detected, respectively, by H&E and EVG. Magnification: $\times 200$. CPs indicates cardiac pericytes; EVG, Elastic Van Gieson staining; H&E, hematoxylin and eosin.

ylin and eosin) and for the extracellular matrix components elastin and collagen (Elastic Van Gieson staining) (Figure 8); in addition, maintenance of the original phenotype was documented by fluorescence staining with vimentin, NG2, and PDGFR β antibodies (Figure 9). Cell viability within the engineered scaffold was confirmed with live-cells imaging using the Biotium viability/cytotoxicity Assay kit (Figure 10).

Discussion

Clinical cell therapy for heart disease has been aimed at promoting the healing of ischemic myocardium in adult patients. New evidence suggests that SC therapy could potentially offer a new treatment standard for patients with CHD.²⁷ Importantly, the neonatal heart offers a wider and more naïve spectrum of cellular options than the adult heart.

The field is still in its beginning, with initial clinical studies showing evidence of feasibility and safety.²⁸

Here, we show new data on progenitor cells that could be considered for tissue engineering in patients with CHD. Using a standard operating procedure previously set up to obtain pericytes from human saphenous veins, we have now isolated, expanded, and characterized a novel population of CPs from both atria and ventricle of infants and children with CHD.

The idea of “recycling” and expanding regenerative cells from tiny surplus material of palliative surgery suggests a sustainable therapeutic undertaking. The reported expansion success (≈ 20 million cells at P5, in 4 to 6 weeks in 77% of samples examined) largely surpasses the outcome previously obtained with saphenous vein leftovers.¹⁶ This may be due to either a greater abundance or higher proliferation rate of founder cells from the neonatal heart as compared with counterpart cells from the adult vasculature. The higher expression of SC markers by, and greater clonogenic activity of, cardiac versus vascular pericytes suggests that the former are more immature elements capable of high expansion capacity. Furthermore, CPs have the ability to differentiate into VSMCs under *in vitro* inductive conditions, whereas this property was lacking in adult vascular pericytes.¹⁶ However, analysis of specification into other cardiovascular lineages indicates a relative restriction of CP differentiation capacity. In fact, they do not express typical EC markers before and after stimulation by endothelial inducers. Additionally, the incomplete manifestation of cardiac transcription factors/protein combined with lack of developing electrophysiological properties of mature cardiomyocytes indicates the incapacity of CPs to transverse the whole cardiomyogenic process. The measurement of membrane current and intracellular Ca^{2+} shows the feasibility of making such measurements from neonatal CPs. These experiments also show that expansion results in cells that exhibit transmembrane ion flux, which does not change linearly with voltage, and thus appears to be presumably controlled by ion channels in the cell membrane. The voltage dependence of membrane current indicates a nonspecific cation conductance, as described previously in other pericyte populations.²⁹ Similarly, the observation, in agreement with previous work,²⁹ that IP_3 can cause an increase of intracellular Ca^{2+} indicates that pericytes have intracellular Ca^{2+} handling mechanisms, including the ability to sequester Ca^{2+} into an intracellular organelle, from which it can be released, presumably via IP_3 receptors. However, the lack of Ca^{2+} and Na^+ currents, and the inability of electrical stimulation to cause an increase of intracellular Ca^{2+} , show that these cells differ from electrically excitable cells, such as cardiomyocytes. The differentiation protocol used in the present study appeared to have no effect on membrane currents, although the ability of IP_3 to release intracellular

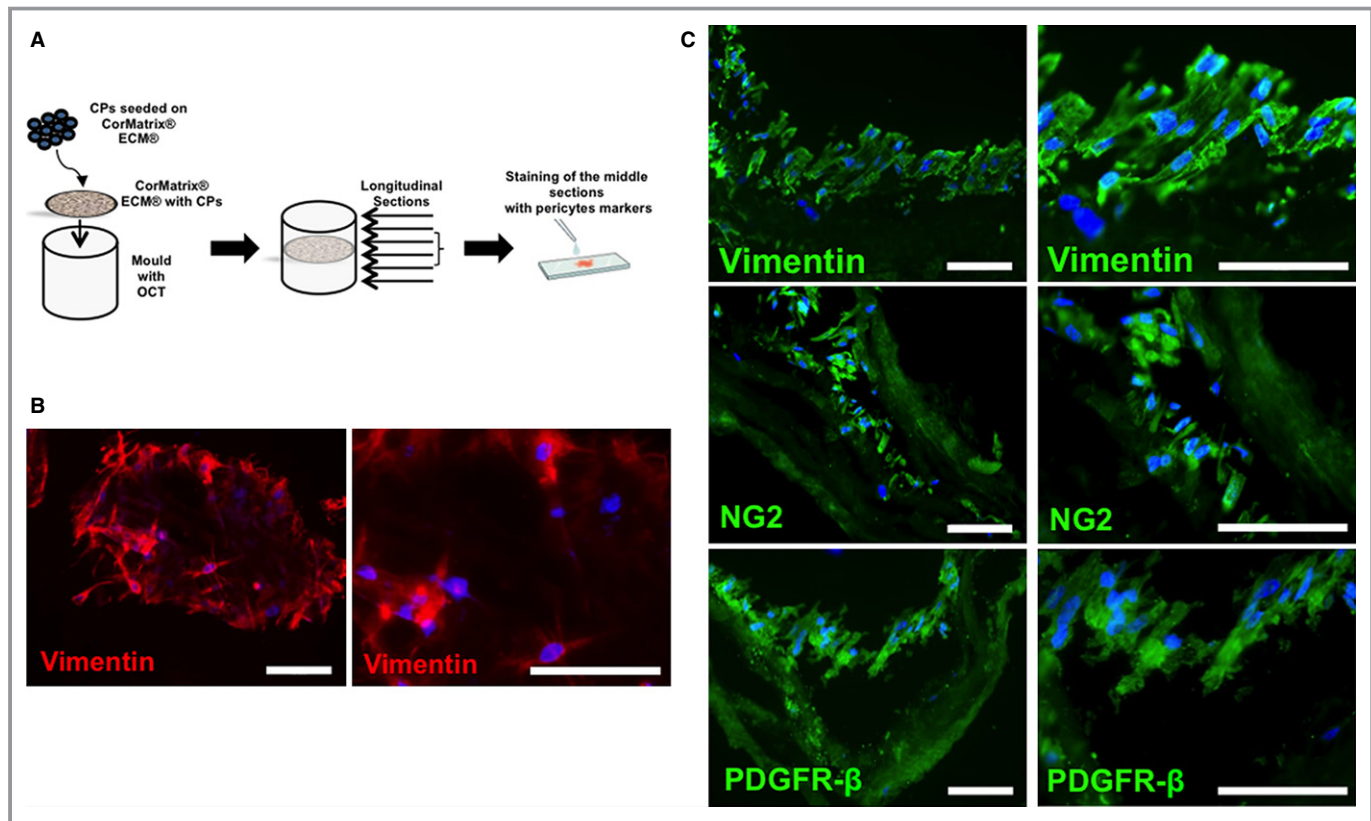


Figure 9. CPs engraft in the CorMatrix. CPs (P5) were seeded onto CorMatrix[®] ECM[®]. After culturing the bioscaffolds with CPs in EGM2 for 1 week in static conditions and 2 weeks in dynamic conditions (within a bioreactor), they were included in molds with O.C.T. Compound, Tissue-Tek (OCT) as depicted in the schematic figure (A). After 24 hours in the freezer, longitudinal sections were cut from the OCT blocks containing the bioscaffolds. Sections from the middle of these samples were stained with pericyte markers anti-vimentin, anti-NG2, and anti-PDGFR- β antibodies to check for the presence of CPs inside the bioscaffolds both in static (B) and dynamic conditions (C). In (C), the figures in the right panel are shown with higher magnification for better observation of CPs engrafted within the graft. Nuclei were counterstained with DAPI. Scale bar: 100 μ m. CPs indicates cardiac pericytes; DAPI, 4',6-diamidino-2-phenylindole; ECM, extracellular matrix; EGM2, endothelial growth medium 2; NG2, neural/glial antigen 2; PDGFR- β , platelet-derived growth factor receptor- β .

Ca²⁺ stores appeared to be lost, and the lack of response to caffeine suggests absence of Ca²⁺ release from intracellular stores via ryanodine receptors (the normal mechanism for Ca²⁺ release in cardiac myocytes, in response to transmembrane Ca²⁺ influx).

Our results are apparently at variance with the findings of Chen et al,¹⁴ who showed that a small fraction of CD146^{pos} pericytes manifest a cardiomyogenic potential following a pulse 5-azacytidine treatment and coculture in vitro with neonatal cardiomyocytes. We used 2 protocols for induction of cardiomyocyte differentiation, including 1 that employs 5-azacytidine as an epigenetic modifier favoring differentiation. The use of cardiomyocytes in coculture might have helped the cardiomyogenic induction of CD146^{pos} pericytes; however, as stated by Chen et al, the possibility of fusion of pericytes with feeder cells cannot be excluded. Moreover, given that Chen and colleagues worked on cardiac biopsies that were obtained postmortem from subjects that had died from noncardiac causes, we cannot exclude the possibility

that differences in cell behavior could be associated with the heart conditions and/or with the standard operating procedure. While we processed our samples immediately after harvesting, it is conceivable the necrosis in samples might have been present for a longer time before reaching the tissue culture laboratory and the undefined causes of death might have affected the epigenetic and molecular signature in Chen's samples.

Although unable to differentiate in ECs and cardiomyocytes, CPs possess other reconstitutive properties that make them relevant for tissue repair and engineering. We show that CPs exert chemoattractive activity toward ECs and form tubular networks in Matrigel alone and in a cooperative fashion with ECs. They also produce large amounts of growth factors and cytokines implicated in angiogenesis. Additionally, CP conditioned media remarkably stimulate the recruitment of human CSCs. CPs also release procollagen type 1, a major constituent of cardiac extracellular matrix.

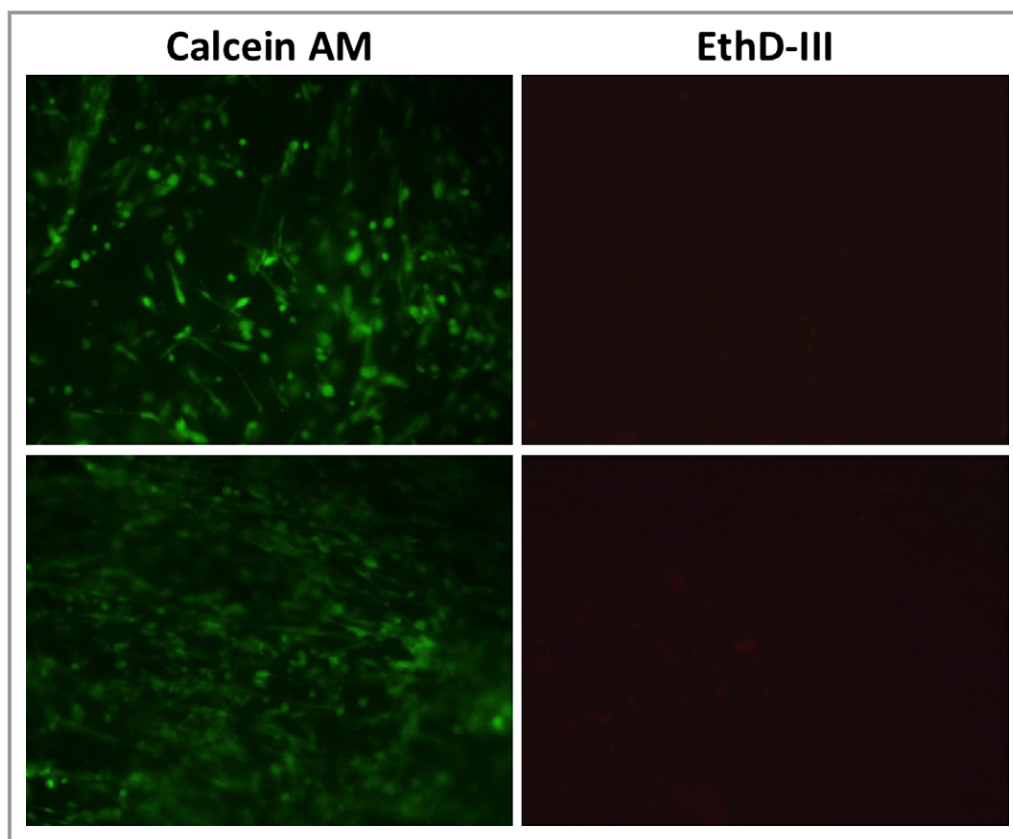


Figure 10. Live-cells imaging analysis of cardiac pericytes viability within the CorMatrix scaffold cultured in the bioreactor. The viability of the cells seeded onto the scaffold was detected using the Biotium viability/cytotoxicity Assay kit. In representative fluorescence images, live cells are indicated by the cytoplasmic green fluorescence of Calcein AM, while very rare dead cells are detectable by the nuclear red fluorescence of EthD-III. Magnification: $\times 100$.

Finally, in view of creating a pericyte-engineered graft for correction of congenital heart defects, we seeded CPs in a xenograft scaffold under static and dynamic conditions. Engineering of prosthetic grafts with autologous SCs has the 2-fold aim of reducing the thrombogenic risk through re-endothelialization of the graft's luminal surface and conferring the properties of a living tissue that grows and remodels in a physiologic manner in parallel with cardiac and whole body growth. Results show that CPs are able to penetrate deeply within the graft texture after 3 weeks of culture in a bioreactor system, and that cells within the graft are viable. Moreover, cells maintain the original antigenic phenotype.

With respect to other competing/complementary solutions for cellularization of cardiac grafts, CPs appear to be a more refined and safer cell therapy product. For instance, CPs can be isolated/expanded from the tiny discarded tissue (<100 mg) obtained at palliative CHD surgery, whereas the scarcity of other SCs in the heart precludes this possibility. Moreover, pericytes do not induce calcification when implanted in the heart of mice, as observed with mesenchymal SCs.¹⁹ CPs may be preferred to pericytes from other

organs, because the former do not require an elective harvesting procedure and are assumed to engraft more efficiently in their native tissue. A recent clinical trial showed the feasibility, safety, and therapeutic efficacy of intracoronary administration of autologous cardiosphere-derived cells in children with hypoplastic left heart syndrome.²⁸ Comparison of CPs and cardiosphere-derived cells indicates some similarities, as both cell populations express CD105, CD90, vimentin, and GATA4 and are negative for CD31 and CD45. However, different from cardiosphere-derived cells, CPs do not express Tbx5, NKX2.5, and FLK1. Furthermore, cardiosphere-derived cells classically express c-Kit,²⁴ which is instead absent in CPs. Therefore, the 2 cell types may represent distinct and potentially complementary therapeutic elements within the pool of cardiac SCs.

In conclusion, we provide a method to isolate and expand a unique population of pericytes from surgery remnants of congenitally defective hearts. This is of high clinical relevance because the starting material is usually available during palliative surgery without additional risk or burden to the patient. The method allows easy preparation and

expansion of the cells to provide elements that accomplish important requirements for cell therapy and tissue engineering, being expandable in vitro and able to produce essential extracellular protein and angiogenic factors, stimulate angiogenesis, attract CSCs, and engraft into biodegradable prosthetic material with high efficiency. Pericyte-engineered grafts could be prepared using a good manufacturing practices-compliant protocol at the time of the first operation in patients born with tetralogy of Fallot or the more severe variant of pulmonary atresia (usually a palliative procedure such as a shunt) using a small amount of tissue collected from the right atrium. The tissue-engineered grafts will then be ready for implantation within the 3- to 4-month gap that normally separates the palliative operation at birth with the final complete surgical correction. Although a long multistep procedure is required to test the good manufacturing practices quality of a cellular product in order to reach clinical applicability, including preclinical in vivo studies in animal models of CHD, with this first study we aimed at demonstrating the feasibility of isolating and expanding several million of CPs from tiny myocardial samples of the youngest patients, and their properties that may elect CPs as good candidates for use in reconstructive surgery. Currently, the scarce availability of commercial animal models of complex CHD limits the possibility of testing the in vivo regenerative ability of CPs, but our surgical team is working in this direction. Indeed, our next step will be represented by feasibility studies with CPs in an animal model of CHD. This approach may open new avenues for correction of complex congenital cardiac defects with immense medical and social benefits.

Acknowledgments

We are thankful to the Wolfson Bioimaging Facility of the University of Bristol for the use of the confocal microscopes.

Sources of Funding

This work was supported by (1) manufacture scaleup of human pericyte progenitor cells for regenerative medicine, MRC Translational Stem Cell Research Grant; (2) Bristol Biomedical Research Unit in Cardiovascular Disease (lead for Regenerative Medicine workpackage), National Institute Health Research Biomedical Research Unit (NIHR BRU); (3) preclinical trial with human pericyte progenitors in a large animal model of myocardial infarction, BHF special project grant; (4) BHF Centre of Regenerative Medicine; and (5) the Sir Jules Thorn award 2014.

Disclosures

None.

References

1. Khoshnood B, Lelong N, Houyel L, Thieulin AC, Jouannic JM, Magnier S, Delezoide AL, Magny JF, Rambaud C, Bonnet D, Goffinet F, Group ES. Prevalence, timing of diagnosis and mortality of newborns with congenital heart defects: a population-based study. *Heart*. 2012;98:1667–1673.
2. Tennant PW, Pearce MS, Bythell M, Rankin J. 20-year survival of children born with congenital anomalies: a population-based study. *Lancet*. 2010;375:649–656.
3. McElhinney DB. Recent progress in the understanding and management of postoperative right ventricular outflow tract dysfunction in patients with congenital heart disease. *Circulation*. 2012;125:e595–e599.
4. Tweddell JS, Pelech AN, Frommelt PC, Mussatto KA, Wyman JD, Fedderly RT, Berger S, Frommelt MA, Lewis DA, Friedberg DZ, Thomas JP Jr, Sachdeva R, Litwin SB. Factors affecting longevity of homograft valves used in right ventricular outflow tract reconstruction for congenital heart disease. *Circulation*. 2000;102:III130–III135.
5. Bernstein HS, Srivastava D. Stem cell therapy for cardiac disease. *Pediatr Res*. 2012;71:491–499.
6. Pincott ES, Burch M. Potential for stem cell use in congenital heart disease. *Future Cardiol*. 2012;8:161–169.
7. Scholl FG, Boucek MM, Chan KC, Valdes-Cruz L, Perryman R. Preliminary experience with cardiac reconstruction using decellularized porcine extracellular matrix scaffold: human applications in congenital heart disease. *World J Pediatr Congenit Heart Surg*. 2010;1:132–136.
8. Bertipaglia B, Ortolani F, Petrelli L, Gerosa G, Spina M, Pauletto P, Casarotto D, Marchini M, Sartore S; Vitalitate Exornatum Succedaneum Aorticum Labore Ingenioso Obtenibitur P. Cell characterization of porcine aortic valve and decellularized leaflets repopulated with aortic valve interstitial cells: the VESALIO Project (Vitalitate Exornatum Succedaneum Aorticum Labore Ingenioso Obtenibitur). *Ann Thorac Surg*. 2003;75:1274–1282.
9. Hibino N, McGillicuddy E, Matsumura G, Ichihara Y, Naito Y, Breuer C, Shinoka T. Late-term results of tissue-engineered vascular grafts in humans. *J Thorac Cardiovasc Surg*. 2010;139:431–436, 436.e1–2.
10. Cebotari S, Tudorache I, Schilling T, Haverich A. Heart valve and myocardial tissue engineering. *Herz*. 2010;35:334–341.
11. Dohmen PM, Lembcke A, Holinski S, Pruss A, Konertz W. Ten years of clinical results with a tissue-engineered pulmonary valve. *Ann Thorac Surg*. 2011;92:1308–1314.
12. Vono R, Spinetti G, Gubernator M, Madeddu P. What's new in regenerative medicine: split up of the mesenchymal stem cell family promises new hope for cardiovascular repair. *J Cardiovasc Transl Res*. 2012;5:689–699.
13. Nees S, Weiss DR, Juchem G. Focus on cardiac pericytes. *Pflugers Arch*. 2013;465:779–787.
14. Chen WC, Baily JE, Corselli M, Diaz M, Sun B, Xiang G, Gray GA, Huard J, Peault B. Human myocardial pericytes: multipotent mesodermal precursors exhibiting cardiac specificity. *Stem Cells*. 2015;33:557–573.
15. Invernici G, Emanuelli C, Madeddu P, Cristini S, Gadau S, Benetti A, Ciusani E, Stassi G, Siragusa M, Nicosia R, Peschle C, Fascio U, Colombo A, Rizzuti T, Parati E, Alessandri G. Human fetal aorta contains vascular progenitor cells capable of inducing vasculogenesis, angiogenesis, and myogenesis in vitro and in a murine model of peripheral ischemia. *Am J Pathol*. 2007;170:1879–1892.
16. Campagnolo P, Cesselli D, Al Haj Zen A, Beltrami AP, Krankel N, Katare R, Angelini G, Emanuelli C, Madeddu P. Human adult vena saphena contains perivascular progenitor cells endowed with clonogenic and proangiogenic potential. *Circulation*. 2010;121:1735–1745.
17. Klein D, Weisshardt P, Kleff V, Jastrow H, Jakob HG, Ergun S. Vascular wall-resident CD44+ multipotent stem cells give rise to pericytes and smooth muscle cells and contribute to new vessel maturation. *PLoS One*. 2011;6:e20540.
18. Crisan M, Yap S, Casteilla L, Chen CW, Corselli M, Park TS, Andriolo G, Sun B, Zheng B, Zhang L, Norotte C, Teng PN, Traas J, Schugar R, Deasy BM, Badylak S, Bhurinj HJ, Giacobino JP, Lazzari L, Huard J, Peault B. A perivascular origin for mesenchymal stem cells in multiple human organs. *Cell Stem Cell*. 2008;3:301–313.
19. Katare R, Riu F, Mitchell K, Gubernator M, Campagnolo P, Cui Y, Fortunato O, Avolio E, Cesselli D, Beltrami AP, Angelini G, Emanuelli C, Madeddu P. Transplantation of human pericyte progenitor cells improves the repair of infarcted heart through activation of an angiogenic program involving micro-RNA-132. *Circ Res*. 2011;109:894–906.
20. Beltrami AP, Cesselli D, Bergamin N, Marcon P, Rigo S, Puppato E, D'Aurizio F, Verardo R, Piazza S, Pignatelli A, Poz A, Baccharani U, Damiani D, Fanin R, Mariuzzi L, Finato N, Masolini P, Burelli S, Belluzzi O, Schneider C, Beltrami CA. Multipotent cells can be generated in vitro from several adult human organs (heart, liver, and bone marrow). *Blood*. 2007;110:3438–3446.

21. Smits AM, van Vliet P, Metz CH, Korfage T, Sluijter JP, Doevendans PA, Goumans MJ. Human cardiomyocyte progenitor cells differentiate into functional mature cardiomyocytes: an in vitro model for studying human cardiac physiology and pathophysiology. *Nat Protoc*. 2009;4:232–243.
22. Cheng H, Lederer WJ, Cannell MB. Calcium sparks: elementary events underlying excitation-contraction coupling in heart muscle. *Science*. 1993;262:740–744.
23. Chugh AR, Beache GM, Loughran JH, Mewton N, Elmore JB, Kajstura J, Pappas P, Tatroles A, Stoddard MF, Lima JA, Slaughter MS, Anversa P, Bolli R. Administration of cardiac stem cells in patients with ischemic cardiomyopathy: the SCIPIO trial: surgical aspects and interim analysis of myocardial function and viability by magnetic resonance. *Circulation*. 2012;126:S54–S64.
24. Malliaras K, Makkar RR, Smith RR, Cheng K, Wu E, Bonow RO, Marban L, Mendizabal A, Cingolani E, Johnston PV, Gerstenblith G, Schuleri KH, Lardo AC, Marban E. Intracoronary cardiosphere-derived cells after myocardial infarction: evidence of therapeutic regeneration in the final 1-year results of the CADUCEUS trial (CARDiosphere-Derived aUTologous stem CELls to reverse ventricular dysfunction). *J Am Coll Cardiol*. 2014;63:110–122.
25. Wanjare M, Kuo F, Gerecht S. Derivation and maturation of synthetic and contractile vascular smooth muscle cells from human pluripotent stem cells. *Cardiovasc Res*. 2013;97:321–330.
26. Avolio E, Meloni M, Spencer HL, Riu F, Katare R, Mangialardi G, Oikawa A, Rodriguez-Arabaolaza I, Dang Z, Mitchell K, Reni C, Alvino VV, Rowlinson J, Livi U, Cesselli D, Angelini G, Emanuelli C, Beltrami AP, Madeddu P. Combined intramyocardial delivery of human pericytes and cardiac stem cells additively improves the healing of mouse infarcted hearts through stimulation of vascular and muscular repair. *Circ Res*. 2015;116:e81–e94.
27. Wehman B, Kaushal S. The emergence of stem cell therapy for patients with congenital heart disease. *Circ Res*. 2015;116:566–569.
28. Ishigami S, Ohtsuki S, Tarui S, Ousaka D, Eitoku T, Kondo M, Okuyama M, Kobayashi J, Baba K, Arai S, Kawabata T, Yoshizumi K, Tateishi A, Kuroko Y, Iwasaki T, Sato S, Kasahara S, Sano S, Oh H. Intracoronary autologous cardiac progenitor cell transfer in patients with hypoplastic left heart syndrome: the TICAP prospective phase 1 controlled trial. *Circ Res*. 2015;116:653–664.
29. Kawamura H, Kobayashi M, Li Q, Yamanishi S, Katsumura K, Minami M, Wu DM, Puro DG. Effects of angiotensin II on the pericyte-containing microvasculature of the rat retina. *J Physiol*. 2004;561:671–683.